European Center of Nuclear Research

SUMMER STUDENT WORK REPORT

Characterization of Superconducting Cavities for HIE-ISOLDE

Intern: *Martina Martinello*

Main Supervisor: *Walter Venturini*
Second Supervisor: *Irene Mondino*

Summer 2013

Introduction

In this report the radiofrequency measurements done for the superconducting cavities developed at CERN for the HIE-ISOLDE project are analyzed. The purpose of this project is improve the energy of the REX-ISOLDE facility by means of a superconducting LINAC. In this way it will be possible to reach higher accelerating gradients, and so higher particle energies (up to $10MeV/u$). At this purpose the Niobium thin film technology was preferred to the Niobium bulk technology because of the technical advantages like the higher thermal conductivity of Copper and the higher stiffness of the cavities which are less sentitive to mechanical vibrations. The Niobium coating is being optimized on test prototypes which are qualified by RF measurements at cold.

The main method used to characterize the cavity consists in measuring the values of Q factor, in *continuous wave* (CW) mode, for different accelerating fields.

In this report, after a short explanation on how the RF tests are done, a critical analysis of these curves will be performed and two different methods for the error analysis will be shown. Important information about the material are obtained from the measurements of the frequency shift as a function of the temperature, near to the critical temperature of the Niobium film. Two model are implemented, the first to explain the variation of the resonance frequency with the pressure, and the second one to calculate the Niobium film thickness for a sputtered cavity.

Chapter I

QWRs RF test

The first step of a RF test is the measurement of the calibration point, where the parameters Q and E_{Acc} are calculated with the following equations:

$$Q_0 = \omega_0 \tau_L \left(1 + \beta_c + \beta_t\right) \tag{1.1}$$

$$E_{Acc} = \sqrt{\frac{P_C}{k_1} \tau_L \left(1 + \beta_c + \beta_t\right)} \tag{1.2}$$

$$\omega_0 = 2\pi f_0, \quad \beta_c = \frac{1 \pm \sqrt{P_r/P_f}}{1 \mp \sqrt{P_r/P_f}}, \quad \beta_t = \frac{P_t}{P_C} \tag{1.3}$$

where: f_0 is the resonance frequency of the cavity, $\tau_L$is the decay time of the stored energy, k_1 is a constant value equals to $0.207J/(MV/m)^2$, $P_C = P_f - P_r - P_t$ is the power dissipated by the cavity, P_f is the forward power, P_r is the reflected power, P_t is the transmitted power, β_c is the strength of the coupling between the cavity and the input antenna (in case of overcoupling the upper sign must be used and in case of undercoupling the lower sign must be used), β_t is the strength of the coupling between the cavity and the output antenna.

The calibration point measurement allows to obtain the ratio between the stored energy and the transmitted power, i.e. the decay time of the pick-up τ_{pk} :

$$\tau_{pk} = \frac{U}{P_t} = \frac{Q_0 P_C}{\omega_0 P_t} \tag{1.4}$$

This value remains constant during the experiment so knowing τ_{pk} by the calibration point measurement, the other point of the curve are obtained as:

$$Q_0 = \omega_0 \tau_{pk} \frac{P_t^{'}}{P_C^{'}} \tag{1.5}$$

$$E_{Acc} = \sqrt{\frac{\tau_{pk} P_t^{'}}{k_1}} \tag{1.6}$$

The QWRs measured, for the HIE-ISOLDE project, are the following: Q3_4, Q5_1 and QP1_4.

The Niobium film of the cavity Q3_4 is the fourth Niobium film deposited on the Q3 Copper cavity support. The same cavity can be used for many times as the

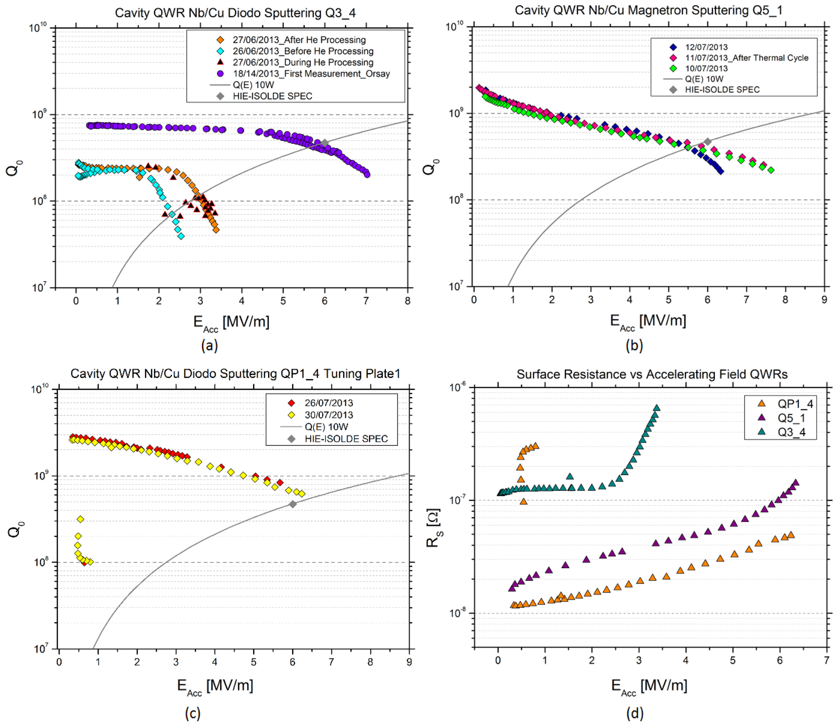

Figure 1.1. Graphs of the unloaded Q-factor versus accelerating field for the: (a) Q3_4 cavity, (b) Q5_1 cavity, (c) QP1_4 cavity. (d) Surface resistance versus accelerating field for the cavity under studied.

Niobium layer can be stripped and re-deposited. The data obtained from the RF test are shown in Fig. 1.1(a); the measurement done in June 2013 at CERN indicates a significant degradation of the RF performance respect to a previous measurement. Further investigations will eventually confirm that the film was damaged during the transport.

The curve of the 26/06/2013 clearly shows that field emission starts at about $2MV/m$: x-rays were detected close to the cavity (max value: $2,3mSV/hr$) and the temperature of the tuning plate increased (it reached $5.337K$). The rise of the temperature on the plate is a proof of field emission since the highest electric field zone is near the inner antenna of the QWR. After the Helium processing the onset of field emission was shifted to higher field ($4MV/m$).

The cavity Q5_1 was the first Niobium film deposited on this substrate. The data obtained are shown in Fig. 1.1(b). The fist measurement did on the 10/07/2013 shows high Q-values, no signs of field emission and high field reached ($8MV/m$).

The curve measured on the 12/07/2013 shows field emission: the Q decreases exponentially, the field increases slowly and a peak of $28mSV/hr$ of radiation was detected outside the cryostat. The maximum accelerating field reached by the cavity was of about $7MV/m$.

The Niobium film of QP1_4 cavity was sputtered with similar deposition parameters as Q3_4. A movable tuning plate in Copper Berillium was mounted, while Q5_1 and Q3_4 had a flat fixed plate.

Looking at the graph in Fig. 1.1(c) a Q-switch appears, this phenomenon could be explained as thermal breakdown due to the tuning plate, which was not able to dissipate the heat like the copper substrate. So after a certain field the temperature of the plate became higher than the critical temperature of Niobium and the power dissipation lowered the intrinsic Q of the cavity.

The Fig. 1.1(d) shows the curves of the surface resistance of the cavity, which is defined as the ratio between the geometrical factor G and the Q-factor, $R_S = G/Q$, versus the accelerating field for the cavity studied. From this graph it is clear that the QP1_4 cavity has the lowest surface resistance value, that falls into the range between 10 and $100n\Omega$. A slightly higher value of surface resistance are shown by Q5_1 cavity, while the cavity Q3_4 shows the worst value of surface resistance that falls into the range between 0.1 and $1\mu\Omega$.

Chapter II
Error Analysis

The error bars in the graph Q_0 versus E_{Acc} were evaluated numerically with a **Montecarlo-like method**. This consists in generating several random numbers, 5000 in this case, with a Gaussian distribution around a real measured value, and with a suitable standard deviation. This random number generation is done for all observables of the experiment, i.e. the attenuation values for reflected, forward and transmitted power, the reflected, forward and transmitted power measured for both the calibration point and each point of the curve, the decay time ($t/2$) and the resonance frequency. The quantities Q_0 and E_{Acc} are calculated with the same formulas used to generate a real graph, but starting from the generated value. In this way one can calculate 5000 values of the final quantities Q_0 and E_{Acc} and the standard deviations that characterize these populations are interpreted as standard uncertainties of these values.

The standard deviations set for each observable are shown in Table 2.1. The standard deviation for the powers depends on the range of the measured value, as indicated in the data sheet of the power meters used (*Rohde & Schwarz NRP-Z11*).

The graph with the error bars obtained are shown in Fig. 2.1(b). The standard deviation found for each point via Montecarlo simulation is quite small and the error increases with the field, because the coupling gets worse at high field since the reflected power increases. In addition the points of the Q-switch have bigger error bars, because, also in this case, the coupling gets worse but now the reflected power increases well over than before.

Table 2.1. Standard deviation values set for the observables of the Q_0 versus E_{Acc} curve.

Quantity	Standard Deviation
$P_{FWD}^{attenuation}$	$0.1[dBm]$
$P_{TXM}^{attenuation}$	$0.1[dBm]$
$P_{RFL}^{attenuation}$	$0.1[dBm]$
$P_{FWD}^{CalPoint}$	$0.077\,or\,0.081[dBm]$
$P_{TXM}^{CalPoint}$	$0.077\,or\,0.081[dBm]$
$P_{RFL}^{CalPoint}$	$0.077\,or\,0.081[dBm]$
P_{FWD}	$0.077\,or\,0.081[dBm]$
P_{TXM}	$0.077\,or\,0.081[dBm]$
P_{RFL}	$0.077\,or\,0.081[dBm]$
t	15
f_0	$1[Hz]$

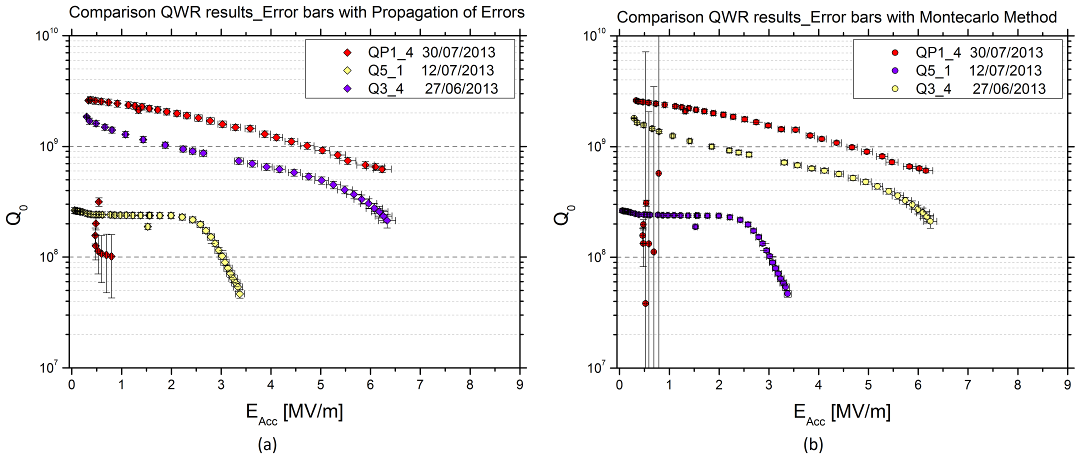

Figure 2.1. Graph of the unloaded Q-factor versus accelerating field with bar errors found via (a) propagation of uncertainty, (b) Montecarlo simulation.

The other method used for calculating the error bars in the graph Q_0 versus E_{Acc} is the **propagation of uncertainty**: it calculates the error propagation for independent variables using the formula proposed by the NIST (National Institute of Standards and Technology) [1]. For a function $f = f(x_1, x_2, ..., x_N)$ one can define the standard deviation of the function as:

$$\sigma_f = \sqrt{\sum_{i=1}^{N} \left(\frac{\partial f}{\partial x_i}\right)^2 \sigma_i^2} \tag{2.1}$$

Where, also in this method, a suitable standard deviation must be defined for each observable. The standard deviations used are the same of the Montecarlo method, shown in Table 2.1.

The graph with the error bars obtained is shown in Fig. 2.1 (a). The standard deviation found for each point via propagation of errors is again quite small and, again, the error increases with the field. The error bars are slightly bigger than the ones found via Montecarlo simulation, but they have the same order of magnitude. So the two methods are consistent. On the other hand, the error bars at the Q-switch found by propagation of errors are smaller than the ones found by Montecarlo simulation, and more trustworthy.

Chapter III
Resonance Frequency Shift Analysis

3.1 Frequency Shift Near the SC Critical Temperature

The frequency variation as a function of temperature was measured for the cavity Q3_4, the curves are shown in Fig. 3.1.

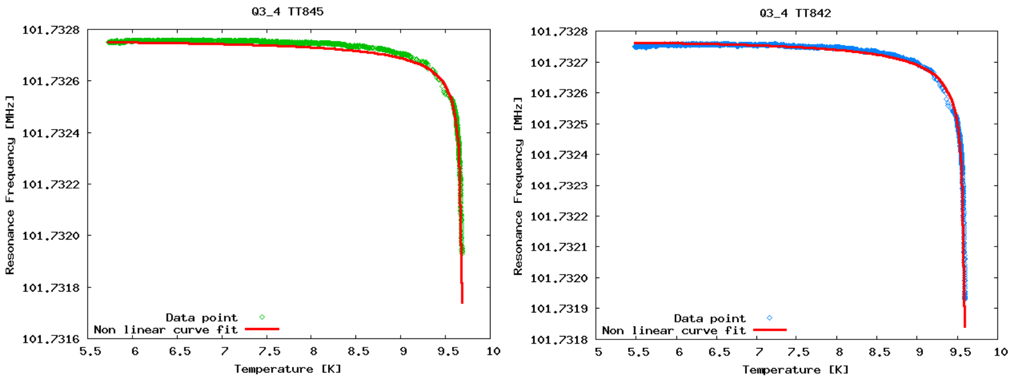

Figure 3.1. Frequency shift near critical temperature as the Q3_4 cavity with the termometers TT845 and TT842.

According to [2], the resonance frequency as a function of temperatures is given by the following equation:

$$f\left(T\right) = f\left(T_{in}\right) + \frac{\pi\mu_0 f_{in}^2}{G - \pi\mu_0 f_{in}\left[\lambda\left(T_{in}\right) - \lambda\left(T_{in}\right)\right]}\left[\lambda\left(T_{in}\right) - \lambda\left(T\right)\right] \tag{3.1}$$

where:$f\left(T_{in}\right)$ is the frequency at the initial temperature T_{in}, μ_0 is the permeability of free space, G is the geometrical factor of the cavity, $\lambda\left(T_{in}\right)$ is the penetration depth at the initial temperature and $\lambda\left(T\right)$ is the penetration depth as a function of temperature, which are defined as [3] :

$$\lambda(T_{in}) = \frac{\lambda_0}{\sqrt{1-\left(\frac{T_{in}}{T_C}\right)^4}}, \quad \lambda(T) = \frac{\lambda_0}{\sqrt{1-\left(\frac{T}{T_C}\right)^4}}, \quad \lambda_0 = \lambda_L\sqrt{1+\frac{\xi_0}{l}} \tag{3.2}$$

where: λ_0 is the penetration depth at $T = 0K$, λ_L is the London penetration depth, ξ_0 is the coherence length, l is the electronic mean free path.

So the data was fitted using the Equation 3.1, setting the following parameter as fixed: T_{in}, $G = 30.32$, $\xi = 64nm$, $\lambda_L = 36nm$ [4] . In this way the parameters T_C, T_{in}, l are given by the fit. Once one has the value of l, it is possible to calculate the impurities contribution to the resistivity, ρ_{imp}:

Table 3.1. Fit results of the frequency shift near the critical temperature data, for Q Q3_4 cavity.

Quantity	Q3_4 TT845			Q3_4 TT831		
$l[nm]$	65	±	1.5	61.0	±	0.8
$T_C[K]$	9.6981	±	0.0003	9.6063	±	0.0002
$f_{in}[MHz]$	101733000.0	±	0.3	101733000.0	±	0.2
$\rho_{imp}[\Omega cm]$	$5.7 \cdot 10^{-7}$	±	$1.3 \cdot 10^{-8}$	$6.07 \cdot 10^{-7}$	±	$8 \cdot 10^{-9}$
RRR	26.5	±	0.6	23.9	±	0.3

$$\rho_{imp} = \frac{1}{l} \frac{m_e v_F}{ne^2} = \frac{1}{l} 0.37 \cdot 10^{-11} \Omega \cdot cm^2 \tag{3.3}$$

where m_e is the electron mass, v_F is the Fermi velocity, n is the free electron density. Now it is also possible to calculate the *Residual Resistivity Ratio*, RRR:

$$RRR = \frac{\rho\,(300K)}{\rho_{imp}} = \frac{\rho_{Ph}\,(300K)}{\rho_{imp}} + 1 \tag{3.4}$$

where ρ_{Ph} is the resistivity due to electron-phonon scattering, for Niobium: $\rho_{Ph}\,(300K) = 15\mu\Omega cm$.

The value obtained are shown in Table 3.1, the calculations made with two different thermometers give different results, because the heating of the cavity is not uniform. The RRR obtained shows that the Niobium thin film analyzed has good proprieties.

3.2 Frequency Shift from Ambient Pressure to Vacuum

There is a difference of about $30kHz$ between the resonance frequency measurement at ambient pressure and in vacuum, at the same temperature. In fact the resonance frequency is defined as:

$$f_0 = \frac{1}{\sqrt{CL}} \tag{3.5}$$

where C is the capacitance and L is the inductance of the cavity. Independently of the shape of the cavity, the capacitance is always directly proportional to the electrical permittivity ϵ. So, the capacitance in vacuum is $C_0 = k\epsilon_0$ and the capacitance at ambient pressure is $C_{Air} = k\epsilon_0\epsilon_r$, making the ratio between the resonance frequency in the two situations, one found:

$$\frac{f_{Air}}{f_0} = \frac{1}{\sqrt{C_{Air}L}} \frac{\sqrt{C_0 L}}{1} = \frac{1}{\sqrt{\epsilon_r}} = \frac{1}{n} \tag{3.6}$$

where ϵ_0 is the vacuum permittivity, ϵ_r is the relative permittivity and n is the refractive index. So the difference between the resonance frequency in vacuum and at ambient pressure is given by:

$$f_0 - f_{Air} = f_0 \left(1 - \frac{f_{Air}}{f_0}\right) = f_0 \left(1 - \frac{1}{n}\right) \tag{3.7}$$

To calculate this quantity it is necessary to find the value of the refractive index of air in the radiofrequency range. This can be done using the Bean-Dutton equation [6] :

$$(n_r - 1)^6 = 77.691\frac{p_d}{T} + 71.97\frac{p_w}{T} + 375406\frac{p_w}{T^2} \tag{3.8}$$

where n_r is the refractive index of radio waves in air, p_d is the dry air pressure in $mbar$, p_w is the partial water vapour pressure in $mbar$, T is the temperature in K. In the case of dry air, at standard condition, with $f_0 = 101MHz$ the results found are:

$$n_r = 1.000288, \quad f_0 - f_{Air} = 0.029MHz \tag{3.9}$$

The frequency shift calculated is in agreement with the experimental data.

It is also possible to model the evolution of the frequency shift from ambient pressure to vacuum pressure. Using the Beam-Dutton model, the variation of the refractive index as a function of the pressure is calculated using the Equation 3.8, while the frequency trend is found out using the following equation:

$$f(p) = \frac{f_0}{n(p)} \tag{3.10}$$

A comparison between the model and the experimental data is shown in Fig. 3.2:

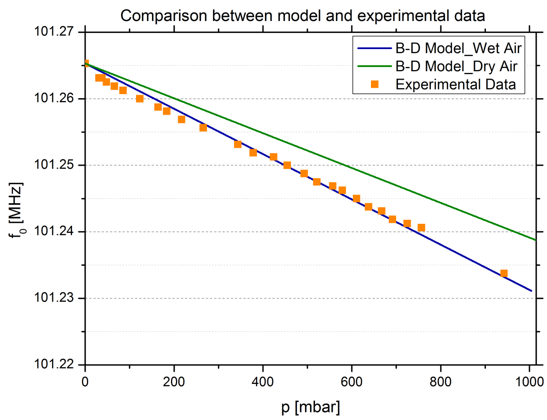

Figure 3.2. Resonance frequency versus pressure: comparison between the experimental and the model data.

The curve obtained for the Bean-Dutton model considering 20% of air humidity fits the experimental data. This model could be useful in order to understand the air humidity, the cavity would became a, quite expensive, hygrometer.

Chapter IV

Warm measurements

4.1 Electrical Proprieties at Room Temperature

At room temperature, about $300K$, the Niobium film of the cavity has normal conductor proprieties, and the Q_L factor can be easily obtained with a network analyzer, from the width of the resonance curve in the frequency domain: $Q_L = \triangle\omega/\omega_0$. In addition the SWR of the coupler can be measured with S_{11} mode and gives directly the value of β. Then it is possible to calculate the unloaded Q factor: $Q_0 = Q_L\,(1+\beta_C)$.

The warm measurement was made for the Niobium thin film cavity, QP1_4, and for a Copper cavity. The results obtained are shown in Table 4.1 .

Table 4.1. Warm Q measurements results for the Niobium thin film cavity and for Copper cavity.

Quantity	Nb/Cu Cavity	Cu Cavity
Q_L	6315	8190
SWR coupling	3.58	2.76
SWR pick-up	/	13.65
Q_0	8075	11770

From the Q factor at room temperature it is possible to obtain some information about the material, like: the surface resistance, the skin depth, the resistivity and the conductivity which are all linked together. The results obtained, starting to the previous results, are shown in Table 4.2 .

Table 4.2. AC proprieties results for the Niobium thin film cavity and for Copper cavity. There are also the AC proprieties found in literature for a case of Niobium cavity.

Quantity	Nb/Cu Cavity	Cu Cavity	Nb Cavity
$R_S[\Omega]$	0.00375	0.00258	0.0076
$\sigma[S/m]$	$2.83 \cdot 10^{7}$	$6.00 \cdot 10^{7}$	$6.90 \cdot 10^{6}$
$\rho[\Omega m]$	$3.54 \cdot 10^{-8}$	$1.67 \cdot 10^{-8}$	$1.45 \cdot 10^{-7}$
$\delta[m]$	$9.42 \cdot 10^{-6}$	$6.46 \cdot 10^{-6}$	$1.91 \cdot 10^{-5}$

In the Nb/Cu cavity $\delta_{eff} = 9.42\mu m$ so if the Niobium film is less thick than this value, the field will pass through the entire film and it will decay in the Copper. The fact that the thickness of the Niobium layer has a lower value than the skin depth is proven by the electrical proprieties: the surface resistance and the resistivity of the Nb/Cu cavity are higher than the Copper cavity but lower than a Niobium one.

4.2 Model for Niobium Average Thickness Calculation

The surface impedance of the Nb/Cu cavity can be defined as:

$$\frac{1}{Z} = \frac{\int_0^a \sigma^{Nb} E\left(z\right)^{Nb}\, dz + \int_0^{+\infty} \sigma^{Cu} E\left(z\right)^{Cu}\, dz}{E_y\left(0\right)} \tag{4.1}$$

in which the electric field into the Niobium film, $E\left(z\right)^{Nb}$, can be defined as [6]

$$E\left(z\right)^{Nb} = E_0 \left[\frac{e^{-(x-a)/\delta} + R \cdot e^{(x-a)/\delta}}{e^{a/\delta} + R \cdot e^{a\delta}}\right] \tag{4.2}$$

where R is the reflection coefficient between the Niobium Copper interface,and is defined as:

$$R = \frac{Z^{Nb} - Z^{Cu}}{Z^{Nb} + Z^{Cu}} = \frac{R_S^{Nb} - R_S^{Cu}}{R_S^{Nb} + R_S^{Cu}} \tag{4.3}$$

It is necessary to take into account the reflected wave from the Nb/Cu interface; a more complete model should also consider the reflected wave from the Nb/air interface and so on, but in this model these contributions are considered negligible.

The first integral of the Equation. 4.1 gives the following result:

$$\int_0^a \sigma^{Nb} E\left(z\right)^{Nb}\, dz = \frac{\sigma^{Nb} E_0}{e^{a/\delta^{Nb}} + R \cdot e^{-a/\delta^{Nb}}} \left[\delta^{Nb}\left(e^{a/\delta} - 1\right) + R \cdot \delta^{Nb}\left(1 - e^{-a/\delta}\right)\right] \tag{4.4}$$

whereas the result of the second integral is:

$$\int_0^{+\infty} \sigma^{Cu} E\left(z\right)^{Cu}\, dz = \sigma^{Cu} E_0 e^{-a/\delta^{Nb}} \int_0^{+\infty} e^{-z/\delta^{Cu}}\, dz = \sigma^{Cu} E_0 \delta^{Cu} e^{-a/\delta^{Nb}} \tag{4.5}$$

So, the surface impedance of the Niobium film on Copper cavity, is:

$$\frac{1}{Z} = \frac{\sigma^{Nb} E_0 \delta^{Nb}}{E_y\left(0\right)} \left[\frac{\left(e^{a/\delta^{Nb}} - 1\right) + R \cdot \left(1 - e^{-a/\delta^{Nb}}\right)}{e^{a/\delta^{Nb}} + R \cdot e^{-a/\delta^{Nb}}}\right] + \frac{\sigma^{Cu} E_0 \delta^{Cu}}{E_y\left(0\right)} e^{-a/\delta^{Nb}} \tag{4.6}$$

And, defining the Copper impedance and the Niobium impedance respectively as:

$$Z^{Cu} = \frac{\sigma^{Cu} E_0 \delta^{Cu}}{E_y\left(0\right)}, \quad Z^{Nb} = \frac{\sigma^{Nb} E_0 \delta^{Nb}}{E_y\left(0\right)} \tag{4.7}$$

one obtains the final result:

$$Q = Q^{Nb} \left[\frac{\left(e^{a/\delta^{Nb}} - 1\right) + R \cdot \left(1 - e^{-a/\delta^{Nb}}\right)}{e^{a/\delta^{Nb}} + R \cdot e^{-a/\delta^{Nb}}}\right] + Q^{Cu} e^{-a/\delta^{Nb}} \tag{4.8}$$

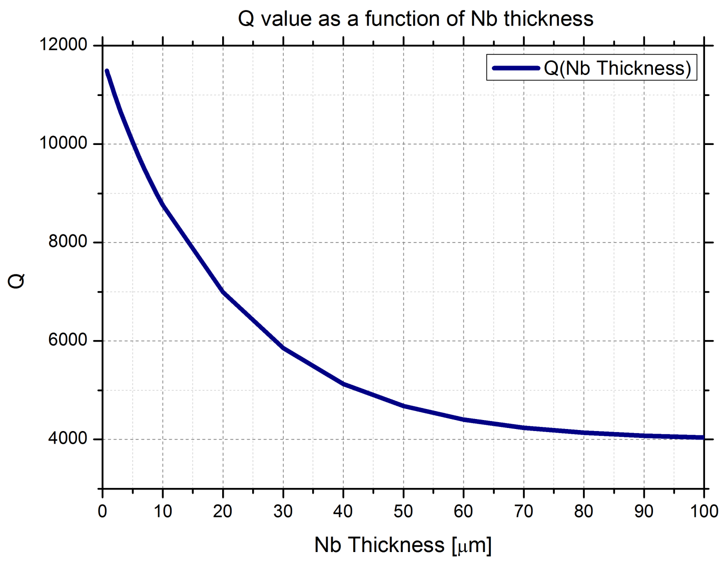

Figure 4.1. Trend of the Q factor of a Niobium thin film on Copper cavity as a function of Niobium thickness.

This equation shows the Q value as a function of Niobium film thickness and the trend found is shown in Fig. 4.1 . A Q factor of 8080 corresponds to a thickness of about 12μm. This value seems overestimated because the thickness should be few *micrometers*. This could be due both to the shape of the QWR and to the non-uniformity of the sputtered Nb layer: in fact the zone of the cavity with the higher losses, where the magnetic field is maximum, is also the zone of the cavity where the film is thicker.

Bibliography

[1] NIST Technical Note 1297: “Guidelines for Evaluating and Expressing the Uncertainty of NIST Measurement Results”, 1994 (http://physics.nist.gov/Pubs/guidelines/TN1297/tn1297s.pdf)

[2] A. D’Elia, ”A methode to evaluate RRR of superconducting cavities” CERN-HIE-ISOLDE-PROJECT-Note-0014, September 2012

[3] C.J. Gorter, H.B.G. Casimir, *Z. Tech. Phys.*, Vol.15, 539 (1934)

[4] J.P. Turneaure, J. Halbritter, H. A. Schwettman *J. Supercond.*, Vol.4,No.5 341 (1991)

[5] J.M. Rüeger *Refractive Index Formulae for Radio Waves*, Proceedings of *FIG XXII International Congress*, Washington, D.C. (2002)

[6] S.M. Wentworth, M.E. Baginski, D.L. Faircloth, S.M. Rao, L.S. Riggs *Calculating Effective Skin Depth for Thin Conductive Sheets*, Proceedings of *IEEE Antennas Prop.*, Albuquerque (2006)